

2-Methoxyestradiol Inhibits Hypoxia-Inducible Factor 1 α , Tumor Growth, and Angiogenesis and Augments Paclitaxel Efficacy in Head and Neck Squamous Cell Carcinoma

Justin L. Ricker,¹ Zhong Chen,¹ Xin Ping Yang,¹ Victor S. Pribluda,² Glenn M. Swartz,² and Carter Van Waes¹

¹Tumor Biology Section, Head and Neck Surgery Branch, National Institute on Deafness and Other Communication Disorders, National Institutes of Health, Bethesda, Maryland; and ²EntreMed, Inc., Rockville, Maryland

ABSTRACT

Purpose: Head and neck squamous cell carcinomas have been reported to overexpress hypoxia-inducible factor (HIF)-1 α , a transcription factor that promotes expression of angiogenesis factors and resistance to programmed and therapy-induced cell death. 2-Methoxyestradiol (2ME2) is a natural compound with HIF-1 α inhibitory activity that is currently being evaluated in phase 1 and 2 clinical trials for advanced solid tumors and multiple myeloma. To our knowledge, this is the first study to evaluate the effects of 2ME2 in head and neck squamous cell carcinoma.

Experimental Design: In the present study, we investigated the effects of 2ME2 alone and in combination with paclitaxel, an active agent in recurrent or advanced head and neck squamous cell carcinoma.

Results: 2ME2 exhibited antiproliferative and cytotoxic effects in a panel of five head and neck squamous cell carcinoma cell lines in the 0.5 to 10 μ mol/L range, including induction of G₂-M blockade, caspase-3/7 activation, and apoptosis at 48 hours. 2ME2 resulted in decreased nuclear HIF-1 α -binding activity and affected the expression of downstream genes, such as *bid*, a proapoptotic bcl-2 family member, and vascular endothelial growth factor, a proangiogenic cytokine. The up-regulation of Bid (57.5% at 12 hours, $P < 0.0006$) and inhibition of vascular endothelial growth factor secretion (57.7% at 24 hours, $P < 0.015$; and 50.3% at 48 hours, $P < 0.0006$) could be partially attributed to the effects on HIF-1 α , because HIF-1 α small interfering

RNAs produced similar effects. Finally, *in vivo*, in a xenograft model of head and neck squamous cell carcinoma using UM-SCC-11A cells, 2ME2 exhibited antitumor and antiangiogenic activity, as measured by CD31 immunostaining.

Conclusions: These results provide support for the use of 2ME2 in combination with paclitaxel for the treatment of recurrent or advanced head and neck squamous cell carcinoma.

INTRODUCTION

Head and neck squamous cell carcinoma affects over 300,000 Americans, with an estimated 29,800 new cases and 8,100 deaths annually (1). Most head and neck squamous cell carcinomas are of advanced stage when diagnosed, and patients with advanced disease are those at greater risk for recurrence. Treatment for locally advanced head and neck squamous cell carcinoma includes surgery and radiation or combination chemotherapy and radiation. Unfortunately, this disease remains difficult to treat; more than one-half of patients with head and neck squamous cell carcinoma die within 5 years of diagnosis, and there has been no significant improvement resulting from newer therapies in the past 30 years.

Tumor hypoxia occurring in advanced head and neck squamous cell carcinoma has been associated with increased angiogenesis and resistance to chemotherapy and radiation treatment (2). In advanced tumors, expression of a number of factors modulating cell survival and angiogenesis are induced by a hypoxic environment as the tumor outstrips its blood supply. Hypoxia-inducible factor (HIF)-1 α , is a transcription factor that is activated under hypoxic conditions and has been shown to be overexpressed in head and neck squamous cell carcinomas (3). Furthermore, HIF-1 α overexpression correlates with mortality and/or treatment failure in head and neck squamous cell carcinomas (4, 5) as well as other cancers (6–8). Genes whose expression is regulated by HIF-1 α include vascular endothelial growth factor (VEGF; ref. 9), a proangiogenic cytokine, and *bid* (10), a proapoptotic bcl-2 family member. We previously reported that VEGF is expressed by head and neck squamous cell carcinomas along with a repertoire of proangiogenic cytokines, including interleukin (IL)-6, IL-8, and GRO-1 (11, 12).

2-Methoxyestradiol (2ME2) is a new agent shown to inhibit activation of HIF-1 α through destabilization of microtubules (13) and has antiproliferative and proapoptotic effects upon various cancer lines *in vitro*. 2ME2 has also shown antitumor and antiangiogenic activities in several preclinical models of cancer (13–19). Evaluation of 2ME2 in clinical trials for the treatment of multiple myeloma, advanced solid tumors, prostate, and metastatic breast cancer is currently underway.

The effects of 2ME2 alone or in combination with agents with activity in head and neck squamous cell carcinoma have

Received 7/15/04; revised 9/2/04; accepted 9/8/04.

Grant support: National Institute on Deafness and Other Communication Disorders Intramural Project DC-00016 (C. Van Waes).

The costs of publication of this article were defrayed in part by the payment of page charges. This article must therefore be hereby marked *advertisement* in accordance with 18 U.S.C. Section 1734 solely to indicate this fact.

Requests for reprints: Carter Van Waes, Tumor Biology Section, Head and Neck Surgery Branch, National Institute on Deafness and Other Communication Disorders, National Institutes of Health, Building 10, Room 5D55, 10 Center Drive MSC-1419, Bethesda, MD 20892. E-mail: vanwaesc@nidcd.nih.gov.

©2004 American Association for Cancer Research.

not been studied. Paclitaxel is an active agent indicated for the treatment of patients with head and neck squamous cell carcinoma (20). Paclitaxel stabilizes the cell cytoskeleton by preventing depolymerization of microtubules, resulting in inhibition of cell division and proliferation and promotion of cell death (21). The objective of this study was to determine whether 2ME2, alone or in combination with paclitaxel, would have antiproliferative, proapoptotic, antitumor, and/or antiangiogenic effects supporting its potential use in the treatment of head and neck squamous cell carcinoma.

MATERIALS AND METHODS

Cell Lines. The squamous cell cancer lines used in these experiments, UM-SCC-1, -6, -11A, -11B and -46, were kindly provided by Dr. T. E. Carey (University of Michigan, Ann Arbor, MI) and were derived from primary human tumors of the head and neck (22). Cells were maintained in Eagle's minimal essential medium supplemented with 10% fetal bovine serum, 50 $\mu\text{g}/\text{mL}$ penicillin/streptomycin, and 2 mmol/L glutamine and incubated at 37°C with 5% CO₂.

Reagents. For *in vitro* studies, 2ME2 was purchased from Sigma Aldrich Co. (St. Louis, MO) and 30 mmol/L stock solutions in dimethyl sulfoxide were made fresh and diluted to the appropriate concentrations in medium. Paclitaxel was also purchased from Sigma Aldrich Co. (St. Louis, MO); and 2 mmol/L stock solutions in dimethyl sulfoxide were aliquoted, stored at -80°C, and diluted to the appropriate concentrations in medium. For *in vivo* studies, a liposomal preparation (di-oleoyl-phosphatidylcholine; Avanti Polar Lipids, Alabaster, AL) of 2ME2 at 20 mg/mL was prepared by EntreMed, Inc. (Rockville, MD).

3-(4,5-Dimethylthiazol-2-yl)-2,5-Diphenyltetrazolium Bromide Assays. UM-SCC-1, -6, -11A, -11B, and -46 cells ($5 \times 10^3/\text{well}$) were grown in 96-well plates and exposed to various concentrations of 2ME2, paclitaxel, or both 24 hours after the cells were plated. Cell proliferation and viability were measured daily for up to 5 consecutive days or at 72 hours after drug treatment using an MTT Cell Proliferation kit (Roche Diagnostics, Indianapolis, IN). Absorbance at 570 nm was determined using a microtiter enzyme-linked immunosorbent assay (ELISA) plate reader.

Caspase Assays. UM-SCC-11A cells ($5 \times 10^3/\text{well}$) were grown in 96-well plates and treated with 2ME2 or vehicle for 48 hours. The cells were then exposed to Z-DEVD-R110 (Promega Corp., Madison, WI) for 1 hour at room temperature. Fluorescence excitation (485 nm) and emission wavelengths (535 nm) were measured using a Wallac Victor² 1420 Multichannel Counter (Perkin-Elmer, Shelton, CT).

Flow Cytometry. UM-SCC-11A cells were grown in T-75 flasks and treated with 2ME2 (10 $\mu\text{mol}/\text{L}$) or vehicle for 48 hours. Cell cycle phase distributions were determined by DNA staining using a CycleTEST PLUS DNA Reagent kit (Becton Dickinson Immunocytometry Systems, San Jose, CA) according to the manufacturer's instructions. In brief, cells were collected and counted, and aliquots containing 5×10^5 cells were treated with trypsin and RNase to digest cellular protein and RNA. The DNA was then stained with propidium iodide and filtered, and the DNA content of 10,000 cells was measured

by flow cytometry (FACScan; Becton Dickinson, San Jose, CA). The percentages of apoptotic and viable cells in each phase of the cell cycle were analyzed by ModFit LT software (Verity Software House, Topsham, ME).

Nuclear Binding Assays. UM-SCC-11A cells were grown to 80% confluence in T-75 flasks and treated with various concentrations of 2ME2 for 24 hours. Nuclear extracts were prepared using a Transfactor Extraction Kit (BD Biosciences Clontech, Palo Alto, CA) according to the manufacturer's instructions. In brief, cells were collected and lysed, and the cytosolic fraction was removed. The nuclear pellets were resuspended and homogenized, and the nuclear extracts were collected. Protein concentrations were determined using a BCA Protein Assay Reagent kit (Pierce, Rockford, IL).

HIF-1 α DNA-binding activity was determined using a BD Mercury TransFactor kit specific for HIF-1 α (BD Biosciences Clontech) according to the manufacturer's instructions. In brief, four 30- μg aliquots of nuclear extracts from each treatment group were added to individual wells of a 96-well plate coated with oligonucleotides containing the consensus-binding sequence of HIF-1 α . Bound HIF-1 α was detected by the appropriate primary and horseradish peroxidase-labeled secondary antibodies. 3,3',5,5'-Tetramethylbenzidine substrate was added and converted by horseradish peroxidase to a blue product. After 30 minutes, the absorbance was measured at 650 nm. Nuclear extracts from Cos-7 cells treated with CoCl₂ (Active Motif, Carlsbad, CA) and nuclear extracts incubated with a HIF-1 α specific competitor oligonucleotide (500 ng) served as positive and negative controls, respectively.

Hypoxia-Inducible Factor 1 α Small Interfering Ribonucleic Acid Transfection. UM-SCC-11A cells were grown to ~75% confluence in T75 flasks and were transfected for 3 hours with either a SMARTpool of small interfering RNAs specific for HIF-1 α (100 nmol/L) or a scrambled control small interfering RNA (100 nmol/L; Dharmacon, Inc., Lafayette, CO) using LipofectAMINE 2000 (Invitrogen, Carlsbad, CA) according to the manufacturer's instructions. Cell culture supernatants were collected 40 hours after the transfection and used for ELISAs.

Enzyme-Linked Immunosorbent Assay. UM-SCC-11A cells ($5 \times 10^4/\text{well}$) were incubated with vehicle or 2ME2 0.6 $\mu\text{mol}/\text{L}$ in 24-well plates. At 24 or 48 hours, cell culture supernatants were collected and centrifuged at 12,000 $\times g$ for 30 minutes at 4°C. ELISAs for VEGF, IL-6, IL-8, and GRO-1 were carried out according to the manufacturer's instructions (R&D Systems, Minneapolis, MN).

Real Time Polymerase Chain Reaction. UM-SCC-11A cells were grown to 75% confluence in T-75 flasks and transfected with HIF-1 α small interfering RNA (100 nmol/L) or exposed to 2ME2 (5 $\mu\text{mol}/\text{L}$) for 4, 8, or 12 hours. The medium was removed, and TRIzol (Invitrogen) was added to lyse the cells. Total RNA was isolated according to the manufacturer's instructions, concentrations were determined by spectrophotometric analysis, and integrity was verified by gel electrophoresis. Single-stranded cDNA was synthesized from total RNA by using High-Capacity cDNA Archive kit (Applied Biosystems, Foster City, CA). Bid and 18S rRNA expression were detected by real time quantitative PCR using the Assays-on-Demand Gene Expression assay. The PCR mixture (30 ng of cDNA in 30

μL of PCR reaction mix) was incubated for 2 minutes at 50°C and 10 minutes at 95°C , amplified 40 cycles for 15 seconds at 95°C , and elongated for 1 minute at 60°C . Thermal cycling and fluorescence detection were performed using an ABI Prism 7700 Sequence Detection System (Applied Biosystems). Relative quantitation of the expression was determined by normalizing the bid signal with the 18S endogenous control. The threshold cycle (CT) numbers were used to calculate the relative expression levels according to the manufacturer's suggested method.

In vivo Tumorigenesis. Female BALB/c-scid mice at 4 to 6 weeks of age were purchased from Division of Cancer Treatment (Frederick, MD). In accordance with NIH guidelines, the mice were housed in a pathogen-free animal facility and treated under a protocol (no. 1102-02) approved by the NIH Animal Care and Use Committee. The mice received subcutaneous inoculations of 5×10^6 UM-SCC-11A cells in the right flank region at 7 weeks of age.

The initial *in vivo* study was undertaken to determine the effects of 2ME2 alone on angiogenesis and tumor growth. The mice were randomized on day 8 into two treatment groups each consisting of 15 mice: vehicle or 2ME2. The mice received intraperitoneal injections of 2ME2 (150 mg/kg) or vehicle (empty liposomes) on days 8 through 12, 15 through 19, and 22 through 24. This dose and daily scheduling were based on previous studies performed at Entremed, Inc. Tumor size and total body weight were measured biweekly by an independent technician in a blinded fashion. Tumor size was calculated as length multiplied by width in millimeters.

To evaluate the effects of 2ME2 in combination with paclitaxel in established head and neck squamous cell carcinoma tumors, a second *in vivo* study was initiated. The mice were randomized, after the tumors were palpable (19 days), based on tumor size into three treatment groups each consisting of 10 mice: vehicle, paclitaxel, or paclitaxel and 2ME2. The mice received vehicle alone or a single intraperitoneal injection of paclitaxel (20 mg/kg on day 20) with or without intraperitoneal injections of 2ME2 (150 mg/kg on days 21-23 and 26-30). Each of the groups had an average tumor size of 5.3 to 5.4 mm^2 on the 19th day after tumor cell inoculation. Tumor size and total body weight were measured as described previously.

Microvessel Density. One day after the treatments were completed, tumors were removed from a subset of mice in the initial *in vivo* study representative of the vehicle or 2ME2 treated groups and fixed in IHC Zinc Fixative (BD Biosciences, San Diego, CA). The tumors were paraffin processed and sectioned (American HistoLabs, Inc., Gaithersburg, MD) for immunohistochemistry. The sections were incubated with rat antimouse CD31 antibody (BD Biosciences; diluted 1:50) or an isotype antibody as a negative control, overnight at 4°C . CD31-positive vessels were visualized using a streptavidin-biotin complex method followed by diaminobenzidine reaction (Vector Laboratories, Inc., Burlingame, CA). The tumor sections were counterstained with hematoxylin to visualize the nuclei. The microvessel density was determined by counting the number of CD31-positive vessels in five high-powered fields ($\times 400$) of each section in a blinded fashion. Three tumors per group were analyzed.

Statistical Analysis. *In vitro* data are shown \pm SD, and *in vivo* data are shown \pm SE. All statistical analysis including correlation coefficient, r , and P values, determined by unpaired t tests, was calculated using Microsoft Excel Analysis ToolPak software (Redmond, WA). $P < 0.05$ was considered to be significant. The R index (RI) was calculated to determine the combinatorial effects of 2ME2 and paclitaxel *in vitro*. In brief, $RI = S_{\text{exp}}/S_{\text{obs}}$, where S_{exp} is the product of the survival observed with drug A and the survival observed with drug B, and S_{obs} is the survival observed with the combination of A and B (23). RI values greater than unity indicate synergism.

RESULTS

2-Methoxyestradiol or Paclitaxel Alone or in Combination Inhibited Head and Neck Squamous Cell Carcinoma Cell Growth. To determine the effects of 2ME2 and paclitaxel on proliferation, human head and neck squamous cell carcinoma lines UM-SCC-1, -6, -11A, -11B, and -46, were exposed to 2ME2 (0-50 $\mu\text{mol/L}$) or paclitaxel (0-1 $\mu\text{mol/L}$) and assayed daily by 3-(4,5-dimethylthiazol-2-yl)-2,5-diphenyltetrazolium bromide until the vehicle-treated cells reached confluence at 4 to 5 days (Fig. 1). Single-agent treatment of 2ME2 or paclitaxel at concentrations similar to those expected in patients resulted in significant antiproliferative activity in all of the cell lines examined. The cell lines displayed $< \log_{10}$ variation in sensitivities to the two agents. The IC_{50} values of 2ME2 in UM-SCC-1, -6, -11A, -11B, and -46 were 0.63, 0.55, 0.74, 1.29, and 0.93 $\mu\text{mol/L}$, respectively. The IC_{50} values of paclitaxel in these same cell lines were 9.7, 14.6, 12.0, 5.9, and 5.8 nmol/L . Interestingly, the sensitivities to the two treatments showed an inverse correlation ($r = -0.82$), suggesting that 2ME2 and paclitaxel in combination may be beneficial in targeting cells less sensitive to either agent alone. The panel of cell lines was then exposed to 2ME2, paclitaxel, or both for 72 hours and assayed by 3-(4,5-dimethylthiazol-2-yl)-2,5-diphenyltetrazolium bromide to determine the effects on proliferation of the combined treatments. The concentrations of 2ME2 or paclitaxel that gave similar inhibition of cell growth in the different cell lines were used. 2ME2 in combination with paclitaxel resulted in additive antiproliferative effects in UM-SCC-6, -11A, and -46, and synergistic antiproliferative effects in UM-SCC-1 ($RI = 1.66$) and -11B ($RI = 2.92$) when compared with 2ME2 or paclitaxel as a single agent.

2-Methoxyestradiol Inhibited Cell Cycle Progression, Induced Sub- G_0/G_1 Fragmentation, and Activated Caspase-3 and Caspase-7 Head and Neck Squamous Cell Carcinoma Cells. After determining that 2ME2 exhibited antiproliferative effects in the panel of cell lines, we investigated the specific effects of 2ME2 on cell cycle progression and apoptosis using DNA flow cytometry. DNA histograms from cells incubated with either vehicle or 2ME2 (10 $\mu\text{mol/L}$) for 48 hours (Fig. 2A and B) revealed that 2ME2 treatment results in G_2 -M blockade (76.01% versus 7.59% in vehicle-treated cells; Fig. 2C) and increased subcellular DNA fragment staining (19.16% versus 0.24% in vehicle-treated cells; Fig. 2D). Interestingly, the fluorescent channel detecting the DNA peak corresponding to G_0 - G_1 shifted from ~ 48 (1N) in the histogram of vehicle-treated cells (Fig. 2A) to ~ 96 (2N) in the histogram of 2ME2-

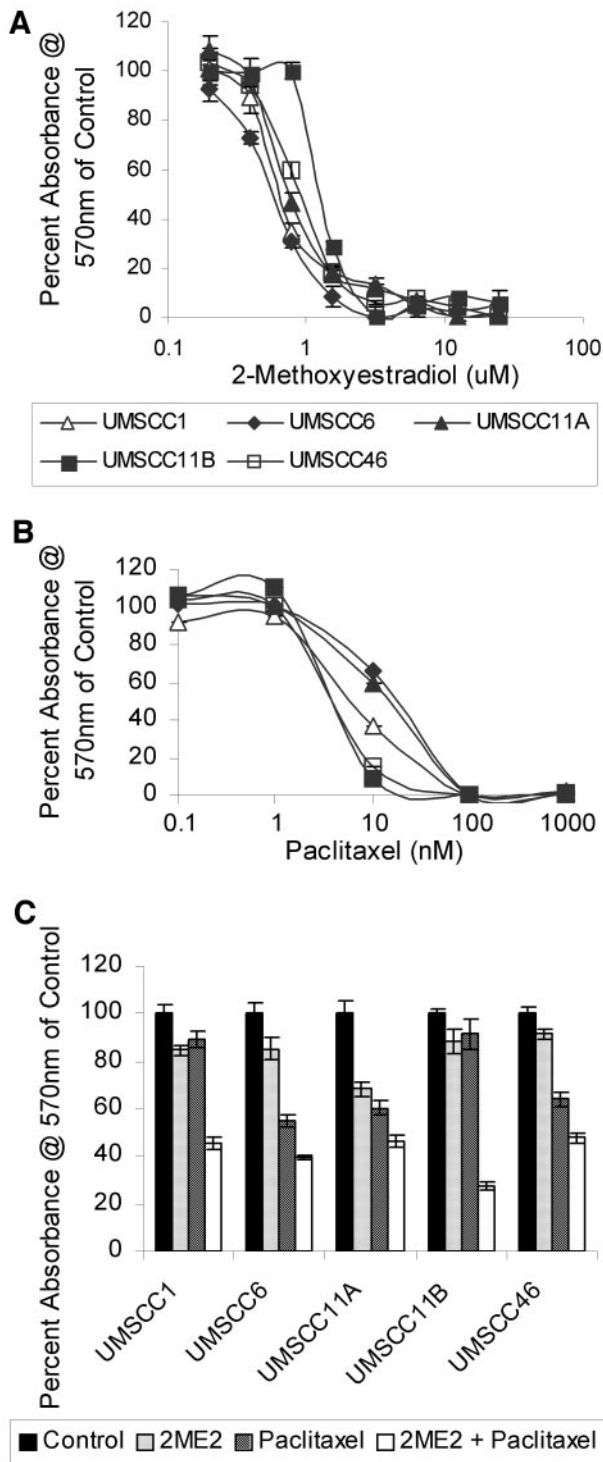


Fig. 1 2ME2 or paclitaxel alone or in combination significantly inhibited head and neck squamous cell carcinoma cell growth. UM-SCC-1, -6, -11A, -11B, and -46 cells (5×10^3 per well) were grown up in 96-well plates and continuously exposed to various concentrations of 2ME2 (A), paclitaxel (B), or both (C) for 72 hours. Six replicates were performed for each data point, and data are shown as mean \pm SD.

treated cells (Fig. 2B). The DNA peak detected at a fluorescent channel of ~ 190 (Fig. 2B), therefore, represents cells undergoing two rounds of DNA synthesis (4N) without mitosis. This conclusion is consistent with the observation that 2ME2-treated cells were much larger than vehicle-treated cells under the microscope (data not shown). To further examine the apoptotic pathway activated by 2ME2, UM-SCC-11A cells were exposed to 2ME2 (0.75 or 1.5 $\mu\text{mol/L}$) for 48 hours and assayed for activated caspase-3/7. Levels of activated caspase-3/7 after 2ME2 exposure at 0.75 and 1.5 $\mu\text{mol/L}$ were 7.4- and 8-fold greater than in the controls (Fig. 2E), implicating activation of effector caspases in 2ME2-mediated apoptosis.

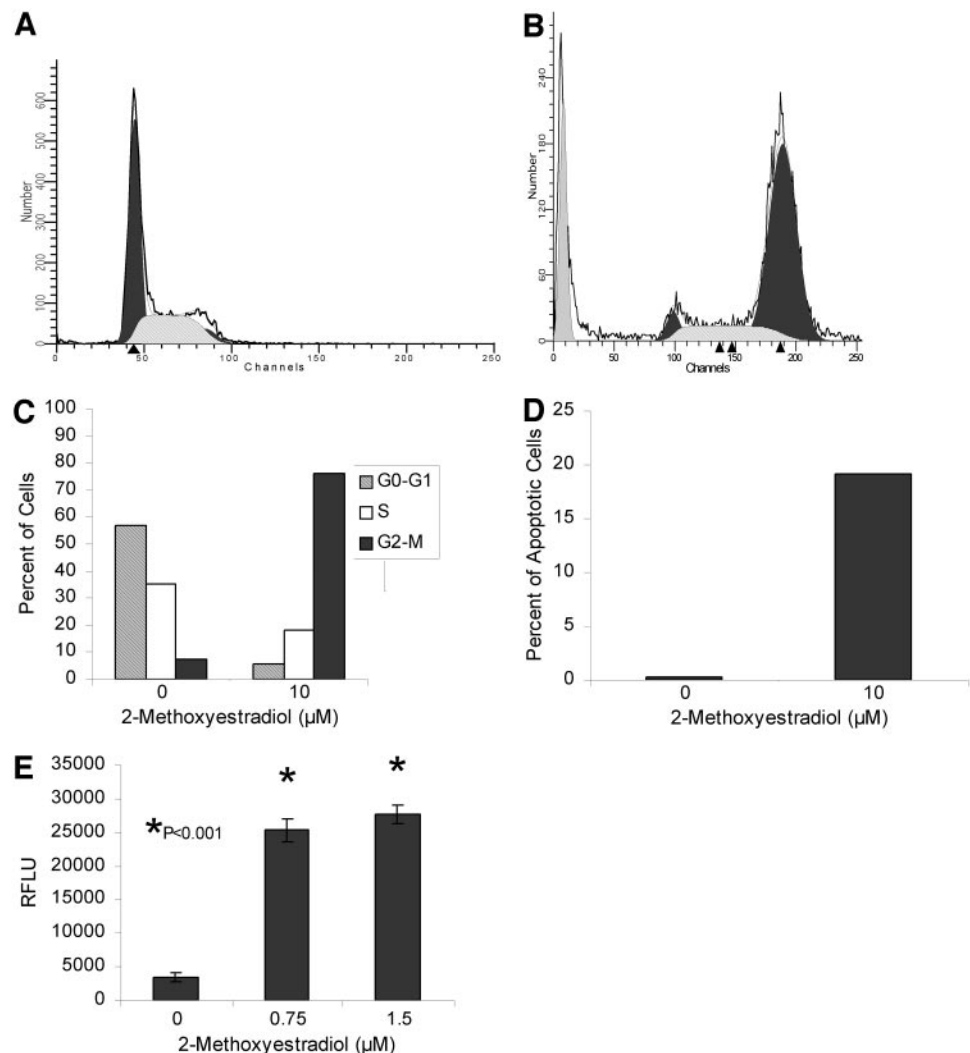
2-Methoxyestradiol Inhibited Hypoxia-Inducible Factor 1 α Activity and Vascular Endothelial Growth Factor Secretion and Promoted Bid Up-regulation. We previously reported that UM-SCC lines secrete angiogenic factors VEGF, IL-6, IL-8, and GRO-1 (11, 12). HIF-1 α is reported to be activated in head and neck squamous cell carcinomas and is a determinant of expression of VEGF (9) and the pro-apoptotic factor bid (10). The effects of 2ME2 treatment on HIF-1 α , angiogenesis factors, and bid expression were evaluated. Nuclear extracts from UM-SCC-11A cells exposed to 2ME2 (0.5, 1.0, 1.5, or 2.0 $\mu\text{mol/L}$) or vehicle for 24 hours were assayed for HIF-1 α -binding activity. 2ME2 treatment resulted in a dose-dependent decrease in nuclear HIF-1 α activity (Fig. 3A). Nuclear extracts from Cos-7 cells treated with CoCl_2 and nuclear extracts incubated with competitor oligonucleotide (500 ng) served as positive and negative controls, respectively.

Angiogenic factor expression was then evaluated in UM-SCC-11A cells exposed to 2ME2. Compared with other head and neck squamous cell carcinoma cell lines, UM-SCC-11A cells are quite aggressive and resistant to various agents (data not shown). This cell line thus served as a realistic model of head and neck squamous cell carcinoma. Cells were incubated with 2ME2 (0.6 $\mu\text{mol/L}$) or vehicle for 24 or 48 hours; and cell supernatant levels of VEGF, IL-6, IL-8, and GRO-1 were analyzed by ELISA. 2ME2 treatment led to a 57.7 and 50.3% decrease in VEGF levels at 24 and 48 hours, respectively (Fig. 3B). 2ME2 did not affect the secreted levels of the other angiogenic cytokines analyzed, including IL-6, IL-8, and GRO-1 (data not shown).

To support the potential role of HIF-1 α inhibition in the decrease of VEGF levels induced by 2ME2, we assessed the role of HIF-1 α in VEGF expression. Cells were transfected with a pool of HIF-1 α specific small interfering RNAs (100 nmol/L) or scrambled small interfering RNAs (100 nmol/L), and cell supernatant VEGF levels were analyzed by ELISA. The HIF-1 α small interfering RNA treatment resulted in a 33.5% decrease in secreted VEGF levels (Fig. 3C), suggesting that the effects of 2ME2 on VEGF could be secondary to the effects on HIF-1 α because direct inhibition of HIF-1 α leads to a decrease in secreted VEGF.

To further elucidate the molecular mechanism responsible for the cytotoxic action of 2ME2, expression of *bid* mRNA was evaluated by real time quantitative PCR. Bid is a proapoptotic bcl-2 family member that was recently shown to be inhibited by HIF-1 α (10). UM-SCC-11A cells were transfected with HIF-1 α small interfering RNA (100 nmol/L) as described previously or exposed to 2ME2 (5 $\mu\text{mol/L}$) for 4,

Fig. 2 2ME2 inhibited cell cycle progression, induced sub-G₀/G₁ fragmentation, and activated caspase-3 and caspase-7 in head and neck squamous cell carcinoma cells. DNA histograms by flow cytometry analysis of DNA from 10,000 UM-SCC-11A cells grown to ~70% confluence after vehicle (A) or 2ME2 (B; 10 μ mol/L) exposure for 48 hours. 2ME2 treatment resulted in G₂-M blockade (C) and a severalfold increase in the number of cells undergoing apoptosis as determined by flow cytometry (D). E. UM-SCC-11A cells (5×10^3 /well) were grown in 96-well plates and exposed to 2ME2 (0.75 and 1.5 μ mol/L) or vehicle for 48 hours. The cells were then exposed to Z-DEVD-R110 for 1 hour, and activation of caspase-3 and caspase-7 was detected via fluorescence measurement. Six replicates were performed for each data point, and the data are shown as mean \pm SD.



8, or 12 hours. 2ME2 or HIF-1 α small interfering RNA treatment resulted in significant up-regulation of *bid* expression at 4, 8, and 12 hours, when the relative expression level of *bid* mRNA is normalized to 18S rRNA for each sample (Fig. 3D). Therefore, the induction of apoptosis by 2ME2 is consistent with its inhibitory effects on HIF-1 α and up-regulation of pro-apoptotic factor *bid*.

Antitumor and Antiangiogenic Effects of 2-Methoxyestradiol Alone or in Combination with Paclitaxel in Head and Neck Squamous Cell Carcinoma Tumor Xenografts. Treatment with a liposomal preparation of 2ME2 (150 mg/kg, intraperitoneally, days 8–12, 15–19, and 22–24) significantly inhibited tumor growth at day 22 (4.07 ± 1.70 versus 14.13 ± 2.99 mm² in mice treated with empty liposomes, $P = 0.008$) and 25 (7.73 ± 2.27 versus 20.95 ± 4.51 mm² in vehicle-treated mice, $P = 0.016$) after tumor cell inoculation (Fig. 4A). 2ME2 also inhibited tumor vessel formation as analyzed by CD31 staining at day 25 (26.13 ± 1.90 versus 10.20 ± 1.00 CD31-positive vessels per high powered field ($\times 400$, $P < 0.001$) after tumor cell inoculation (Fig. 4B–F).

In established head and neck squamous cell carcinoma, paclitaxel (20 mg/kg, intraperitoneally, on day 20) treatment alone did not result in significant inhibition of tumor growth, however, 2ME2 (150 mg/kg, intraperitoneally, days 21–23 and 26–30) in combination with paclitaxel inhibited tumor growth after completion of the dosing regimen (Fig. 5). The mice treated with 2ME2 in combination with paclitaxel had significantly smaller tumors than the vehicle-treated mice (17.50 ± 3.32 versus 34.10 ± 3.65 , $P = 0.0022$) at 30 days after tumor cell inoculation (Fig. 5).

Mice treated with 2ME2 at the dose maximally soluble in the liposomal preparation showed no significant toxicity. As previously reported (19), 2ME2 treatment resulted in a slight and temporary decrease in growth and total body weight (13–15.4%). Coinciding with this difference in body weights, the 2ME2-treated mice also seemed more active. No other toxicities were detected in the treatment group. After completion of the treatment regimen, total body weights were not significantly different between the treated and untreated mice.

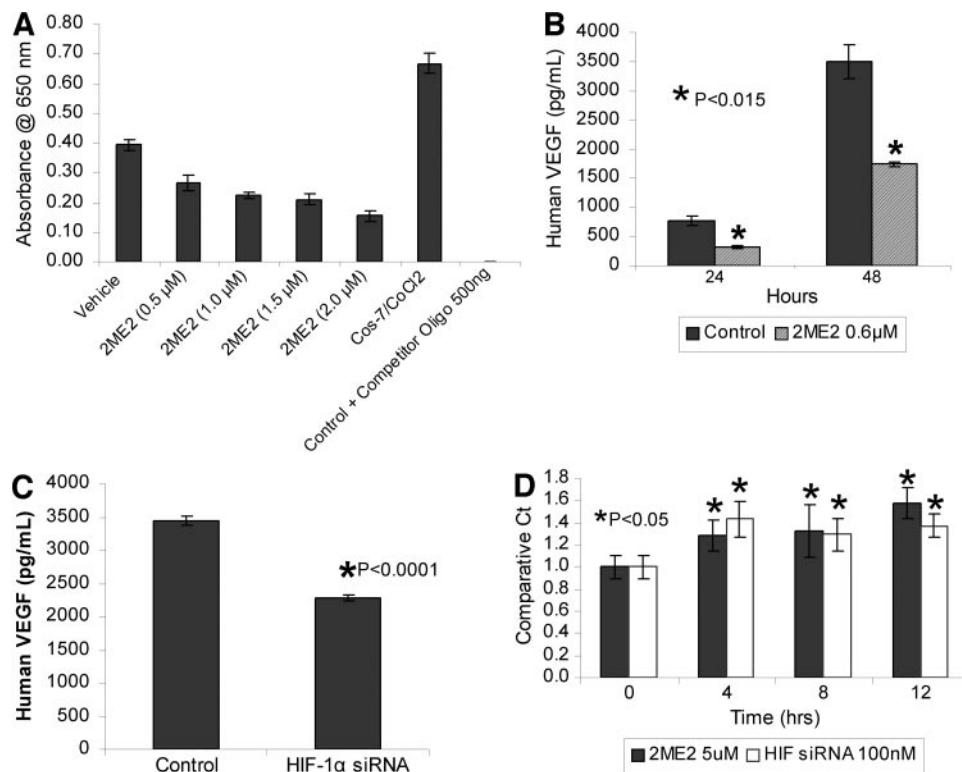


Fig. 3 2ME2 inhibited HIF-1 α activity and VEGF secretion and promoted bid up-regulation. **A.** UM-SCC-11A cells were grown to 80% confluence in T-75 flasks and treated with 2ME2 (0, 0.5, 1.0, 1.5, or 2.0 μ mol/L) for 24 hours. HIF-1 α DNA-binding activity of the nuclear extracts from each treatment group was determined using a BD Mercury TransFactor Kit specific for HIF-1 α . Nuclear extracts from Cos-7 cells treated with CoCl₂ and nuclear extracts incubated with a HIF-1 α -specific competitor oligonucleotide served as positive and negative controls, respectively. **B.** UM-SCC-11A cells (5×10^4 /well) were grown in 24-well plates and exposed to vehicle or 2ME2 0.6 μ mol/L. At 24 or 48 hours, cell culture supernatants were collected and used for VEGF detection by ELISA. **C.** UM-SCC-11A cells were grown to ~75% confluence in T75 flasks and were transfected for 3 hours with either a SMARTpool of small interfering RNAs specific for HIF-1 α (100 nmol/L) or a scrambled control small interfering RNA (100 nmol/L) using LipofectAMINE 2000. Cell culture supernatants were collected 40 hours after the transfection and used for VEGF detection by ELISA. **D.** UM-SCC-11A cells were grown to ~75% confluence in T75 flasks and transfected with HIF-1 α small interfering RNAs or exposed to 2ME2 (5 μ mol/L) for 4, 8, or 12 hours. RNA was isolated, cDNA was synthesized, *bid* and 18S rRNA expression were detected by RT-PCR, and relative *bid* expression was determined by normalizing with the 18S endogenous control. Three or four replicates were performed for each data point, and all data are shown as mean \pm SD.

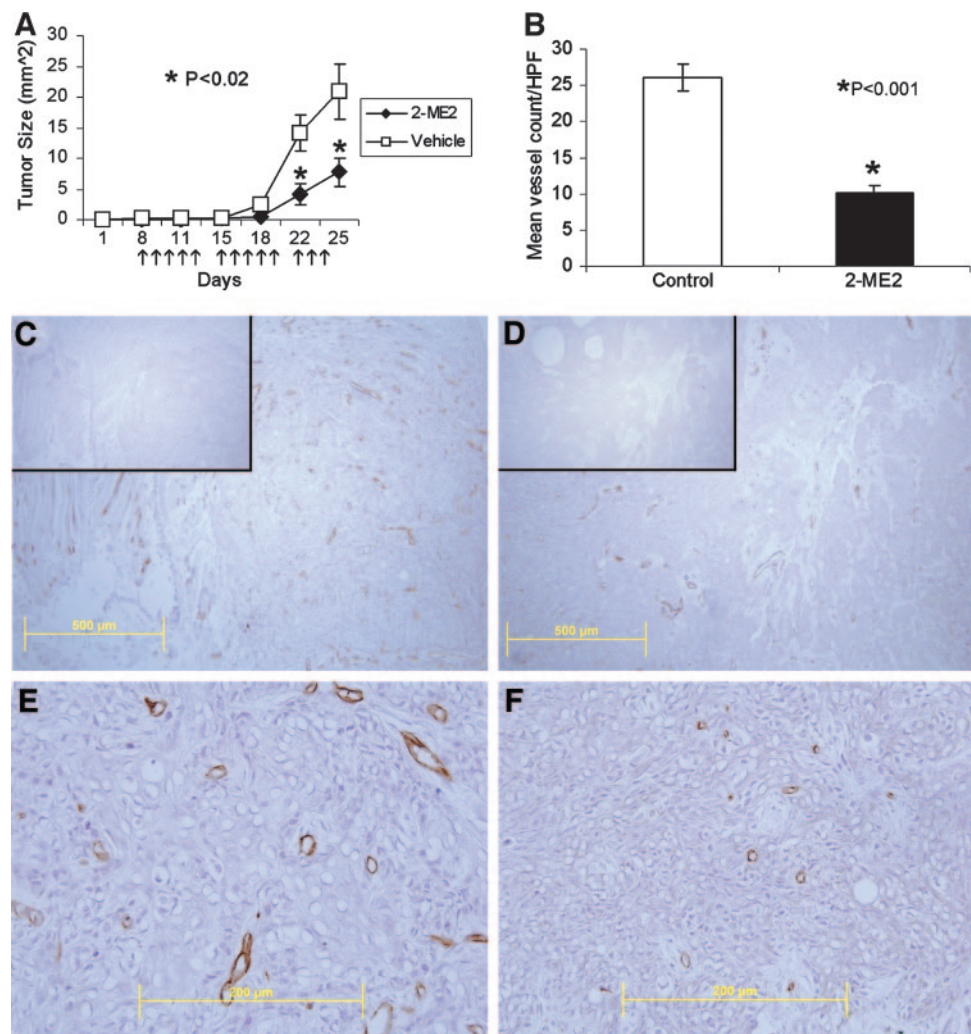
DISCUSSION

The present study revealed that 2ME2 inhibits proliferation and promotes apoptosis of head and neck squamous cell carcinoma lines. 2ME2 also resulted in additive or synergistic antiproliferative activity in combination with paclitaxel *in vitro*. *In vivo*, 2ME2 resulted in significant antiangiogenic and/or antitumor effects alone and in combination with paclitaxel. 2ME2 promoted G₂-M cell cycle block consistent with its effects on microtubules, apoptosis, and angiogenesis. This is consistent with modulation of HIF-1 α and its targets *bid* and VEGF. The effects of 2ME2 on expression of *bid* and VEGF seem to be due, at least in part, to inhibition of HIF-1 α activity, because inhibition of HIF-1 α expression by small interfering RNA also resulted in up-regulation of *bid* and inhibition of VEGF secretion. Bid and VEGF expression may be examined as potential molecular markers for activity in pre- and posttreatment biopsies for patients with oral biopsy-accessible head and neck squamous cell carcinomas enrolled in phase 2 clinical trials using 2ME2 and paclitaxel.

The antiproliferative and apoptotic effects of 2ME2 in head and neck squamous cell carcinoma cell lines are consistent with findings in other cancer types (17, 24–26). An analysis of the cell cycle distribution revealed that 2ME2 inhibited cell cycle progression in the G₂-M phase. 2ME2 has been shown to inhibit progression through mitosis via disruption of microtubule elongation in osteosarcoma (27), uterine sarcoma (28), hepatoma (29), and prostate cancer (13). G₂-M is a radiosensitive phase of the cell cycle, and 2ME2 has shown activity as a radiosensitizer (16, 30). Furthermore, the radiosensitization effects of 2ME2 may be partially dependent on HIF-1 α inhibition (31).

2ME2 inhibited nuclear HIF-1 α activity in a dose-dependent manner. HIF is a heterodimer composed of HIF-1 α and HIF-1 β subunits (32). HIF-1 α is a response factor that is induced by hypoxia, whereas HIF-1 β is an aryl hydrocarbon receptor nuclear translocator that is constitutively expressed. During hypoxia, HIF-1 α binds to hypoxia response elements of HIF-regulated genes. Numerous targets have been identified to date and include VEGF (9), VEGFR1 (FLT-1; ref.33), Bid (10),

Fig. 4 Antitumor and antiangiogenic effects of 2ME2 in head and neck squamous cell carcinoma tumor xenografts. **A**, Mice (15 per treatment group) received empty liposomes or 2ME2 (150 mg/kg) via intraperitoneal injection on days 8 through 12, 15 through 19, and 22 through 24 after tumor cell inoculation as indicated by the arrows. Tumor size (length \times width in millimeters) was measured biweekly by an independent technician in a blinded fashion. **B**, The mean microvessel density for each treatment group was determined by counting the number of CD31-positive vessels in 5 high-powered fields ($\times 400$) of each section in a blinded fashion. Three tumors per group were analyzed. All data are shown as mean \pm SE. **C** and **D**, representative light micrographs of tumor sections from vehicle- or 2ME2-treated mice stained for CD31 1 day after the last treatment. Tumor sections incubated with an isotype antibody (*insets*) served as negative controls to confirm the specificity of the CD31 signal. **E** and **F**, higher magnification light micrographs of tumor sections from vehicle- or 2ME2-treated mice stained for CD31.



TGF- α , UPAR, and MMP-2 (34). In normoxia, HIF-1 α is bound to the VHL tumor suppressor, ubiquitinated, and degraded by the proteasome (35). Loss of heterozygosity of VHL leads to solid tumors including renal cell carcinoma (36). HIF is overexpressed in head and neck squamous cell carcinomas (4, 5) as well as colon, breast, gastric, lung, skin, ovarian, pancreatic, prostate, and renal carcinomas (37). Furthermore, overexpression of HIF correlates with metastasis, decreased response to radiation, chemotherapy, and survival in head and neck squamous cell carcinomas (4, 5).

We show that 2ME2 resulted in a dose-dependent inhibition of nuclear HIF-1 α activity in head and neck squamous cell carcinoma. A previous study has revealed that 2ME2 inhibits HIF-1 α activity in prostate and breast cancer (13). The mechanism by which 2ME2 inactivates HIF-1 α is not fully understood, but recent reports may yield some light on the issue. 2ME2 has been shown to induce superoxide radicals (25), and HIF-1 α is known to be down-regulated by reactive oxygen species (38). We show that 2ME2 affects the expression of the HIF-1 α targets *bid*, a pro-apoptotic bcl-2 family member, and VEGF, a pro-angiogenic cytokine. 2ME2 treatment resulted in

significant up-regulation of *bid* mRNA. This regulation seems to be partially dependent on HIF-1 α activity, because HIF-1 α small interfering RNAs produced similar effects. *Bid* has been shown recently to be down-regulated directly by HIF-1 α in colon cancer cells (10). Furthermore, *bid* overexpression induces apoptosis or sensitizes to chemotherapy induced apoptosis of human cancer cells (39, 40), whereas *bid* knockout mice develop a disorder resembling chronic myelomonocytic leukemia (41). Therefore, *bid* levels are an important factor ultimately regulating survival or death of cancer cells.

2ME2 also resulted in inhibition of the level of secreted VEGF, another target of HIF-1 α . Inhibition of HIF-1 α through transfection with a pool of HIF-1 α small interfering RNAs resulted in a decrease in the level of secreted VEGF. Furthermore, a murine study revealed that knockout of HIF-1 α in teratocarcinomas resulted in retarded tumor growth as well as decreased VEGF secretion during hypoxia (42). 2ME2 has previously been found to inhibit VEGF in breast (13, 15), and pituitary tumors (43) as well as multiple myeloma (18). The lack of effect of 2ME2 on other angiogenic factors such as IL-6, IL-8, and GRO-1 could contribute to the incomplete inhibitory

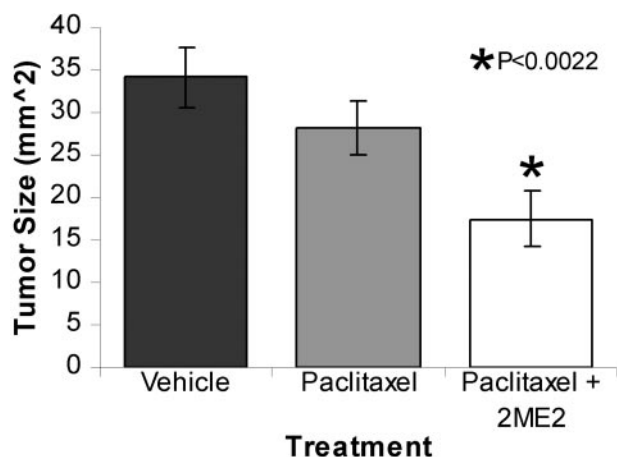


Fig. 5 Antitumor effects of 2ME2 in combination with paclitaxel in established head and neck squamous cell carcinoma tumor xenografts. Mice (10 per treatment group) received empty liposomes, paclitaxel (20 mg/kg on day 20), or paclitaxel in combination with 2ME2 (150 mg/kg on days 21–23 and 26–30 after tumor cell inoculation) via intraperitoneal injection. Tumor size (length \times width in millimeters) was measured by an independent technician in a blinded fashion.

effects on tumorigenesis observed. It will be interesting to determine whether synergism with blockade of these other factors could enhance antiangiogenic and antitumor effects.

In vivo, 2ME2 resulted in significant antiangiogenic and antitumor effects. Anti-angiogenic and antitumor activities of 2ME2 have been observed in other carcinoma models (13–19). Furthermore, 2ME2 in combination with paclitaxel, a first-line treatment for recurrent head and neck squamous cell carcinomas, showed significant antitumor activity during treatment. 2ME2 has previously been shown to exhibit synergy with docetaxel, a related taxane, in breast cancer (44), and this combination was used in a phase I clinical trial for metastatic breast cancer (45). Interestingly, paclitaxel and 2ME2 both induce apoptosis in part through phosphorylation and inhibition of Bcl-xL (46). We believe that the activity exhibited by 2ME2 merits clinical investigation as a new agent in head and neck squamous cell carcinomas, and this study provides support for a clinical trial of 2ME2 in combination with paclitaxel for the treatment of recurrent or advanced head and neck squamous cell carcinomas.

ACKNOWLEDGMENTS

We thank Dr. T. E. Carey for kindly providing us with the cell lines and Dr. Ning Yeh for her lab support.

REFERENCES

- Landis SH, Murray T, Bolden S, Wingo PA. Cancer statistics, 1999. *CA Cancer J Clin* 1999;49:8–31.
- Beasley NJ, Wykoff CC, Watson PH, et al. Carbonic anhydrase IX, an endogenous hypoxia marker, expression in head and neck squamous cell carcinoma and its relationship to hypoxia, necrosis, and microvessel density. *Cancer Res* 2001;61:5262–7.
- Semenza GL. HIF-1 and tumor progression: pathophysiology and therapeutics. *Trends Mol Med* 2002;8(Suppl 4):S62–7.

- Aebersold DM, Burri P, Beer KT, et al. Expression of hypoxia-inducible factor-1 α : a novel predictive and prognostic parameter in the radiotherapy of oropharyngeal cancer. *Cancer Res* 2001;61:2911–6.
- Koukourakis MI, Giatromanolaki A, Sivridis E, et al. Hypoxia-inducible factor (HIF1A and HIF2A), angiogenesis, and chemoradiotherapy outcome of squamous cell head-and-neck cancer. *Int J Radiat Oncol Biol Phys* 2002;53:1192–202.
- Zagzag D, Zhong H, Scalzitti JM, Laughner E, Simons JW, Semenza GL. Expression of hypoxia-inducible factor 1 α in brain tumors: association with angiogenesis, invasion, and progression. *Cancer* 2000;88:2606–18.
- Bos R, van der Groep P, Greijer AE, et al. Levels of hypoxia-inducible factor-1 α independently predict prognosis in patients with lymph node negative breast carcinoma. *Cancer* 2003;97:1573–81.
- Bachtiary B, Schindl M, Potter R, et al. Overexpression of hypoxia-inducible factor 1 α indicates diminished response to radiotherapy and unfavorable prognosis in patients receiving radical radiotherapy for cervical cancer. *Clin Cancer Res* 2003;9:2234–40.
- Forsythe JA, Jiang BH, Iyer NV, et al. Activation of vascular endothelial growth factor gene transcription by hypoxia-inducible factor 1. *Mol Cell Biol* 1996;16:4604–13.
- Erler JT, Cawthorne CJ, Williams KJ, et al. Hypoxia-mediated down-regulation of Bid and Bax in tumors occurs via hypoxia-inducible factor 1-dependent and -independent mechanisms and contributes to drug resistance. *Mol Cell Biol* 2004;24:2875–89.
- Chen Z, Malhotra PS, Thomas GR, et al. Expression of proinflammatory and proangiogenic cytokines in patients with head and neck cancer. *Clin Cancer Res* 1999;5:1369–79.
- Harkins C, Chen Z, Yeh NT, Rudy S, Van Waes C. Serum cytokine levels after therapy as a predictor of prognosis and treatment response in head and neck squamous cell carcinoma [abstract]. Proceedings of the 94th Annual AACR Meeting; 2003 Jul 11–14; Washington, DC. Philadelphia, PA: American Association for Cancer Research; 2003.
- Mabjeesh NJ, Escuin D, LaVallee TM, et al. 2ME2 inhibits tumor growth and angiogenesis by disrupting microtubules and dysregulating HIF. *Cancer Cell* 2003;3:363–75.
- Fotsis T, Zhang Y, Pepper MS, et al. The endogenous oestrogen metabolite 2-methoxyestradiol inhibits angiogenesis and suppresses tumour growth. *Nature* 1994;368:237–9.
- Klauber N, Parangi S, Flynn E, Hamel E, D'Amato RJ. Inhibition of angiogenesis and breast cancer in mice by the microtubule inhibitors 2-methoxyestradiol and Taxol. *Cancer Res* 1997;57:81–6.
- Huober JB, Nakamura S, Meyn R, Roth JA, Mukhopadhyay T. Oral administration of an estrogen metabolite-induced potentiation of radiation antitumor effects in presence of wild-type p53 in non-small-cell lung cancer. *Int J Radiat Oncol Biol Phys* 2000;48:1127–37.
- Schumacher G, Neuhaus P. The physiological estrogen metabolite 2-methoxyestradiol reduces tumor growth and induces apoptosis in human solid tumors. *J Cancer Res Clin Oncol* 2001;127:405–10.
- Chauhan D, Catley L, Hideshima T, et al. 2-Methoxyestradiol overcomes drug resistance in multiple myeloma cells. *Blood* 2002;100:2187–94.
- Dingli D, Timm M, Russell SJ, Witzig TE, Rajkumar SV. Promising preclinical activity of 2-methoxyestradiol in multiple myeloma. *Clin Cancer Res* 2002;8:3948–54.
- Shin DM, Lippman SM. Paclitaxel-based chemotherapy for recurrent and/or metastatic head and neck squamous cell carcinoma: current and future directions. *Semin Oncol* 1999;26:100–5.
- Kumar N. Taxol-induced polymerization of purified tubulin: mechanism of action. *J Biol Chem* 1981;256:10435–41.
- Krause CJ, Carey TE, Ott RW, Hurbis C, McClatchey KD, Regezi JA. Human squamous cell carcinoma: establishment and characterization of new permanent cell lines. *Arch Otolaryngol* 1981;107:703–10.
- Longley DB, Allen WL, McDermott U, et al. The roles of thymidylate synthase and p53 in regulating fas-mediated apoptosis in response to antimetabolites. *Clin Cancer Res* 2004;10:3562–71.

24. LaVallee TM, Zhan XH, Johnson MS, et al. 2-Methoxyestradiol up-regulates death receptor 5 and induces apoptosis through activation of the extrinsic pathway. *Cancer Res* 2003;63:468–75.
25. Chauhan D, Li G, Sattler M, et al. Superoxide-dependent and -independent mitochondrial signaling during apoptosis in multiple myeloma cells. *Oncogene* 2003;22:6296–300.
26. Lambert C, Apel K, Biesalski HK, Frank J. 2-Methoxyestradiol induces caspase-independent, mitochondria-centered apoptosis in DS-sarcoma cells. *Int J Cancer* 2004;108:493–501.
27. Karbowski M, Spodnik JH, Teranishi M, et al. Opposite effects of microtubule-stabilizing and microtubule-destabilizing drugs on biogenesis of mitochondria in mammalian cells. *J Cell Sci* 2001;114:281–91.
28. Amant F, Lottering ML, Joubert A, Thaver V, Vergote I, Lindeque BG. 2-Methoxyestradiol strongly inhibits human uterine sarcomatous cell growth. *Gynecol Oncol* 2003;91:299–308.
29. Lin HL, Liu TY, Chau GY, Lui WY, Chi CW. Comparison of 2-methoxyestradiol-induced, docetaxel-induced, and paclitaxel-induced apoptosis in hepatoma cells and its correlation with reactive oxygen species. *Cancer* 2000;89:983–94.
30. Amorino GP, Freeman ML, Choy H. Enhancement of radiation effects in vitro by the estrogen metabolite 2-methoxyestradiol. *Radiat Res* 2000;153:384–91.
31. Moeller BJ, Cao Y, Li CY, Dewhirst MW. Radiation activates HIF-1 to regulate vascular radiosensitivity in tumors: role of reoxygenation, free radicals, and stress granules. *Cancer Cell* 2004;5:429–41.
32. Wang GL, Semenza GL. Purification and characterization of hypoxia-inducible factor 1. *J Biol Chem* 1995;270:1230–7.
33. Gerber HP, Condorelli F, Park J, Ferrara N. Differential transcriptional regulation of the two vascular endothelial growth factor receptor genes: Flt-1, but not Flk-1/KDR, is up-regulated by hypoxia. *J Biol Chem* 1997;272:23659–67.
34. Krishnamachary B, Berg-Dixon S, Kelly B, et al. Regulation of colon carcinoma cell invasion by hypoxia-inducible factor 1. *Cancer Res* 2003;63:1138–43.
35. Salceda S, Caro J. Hypoxia-inducible factor 1alpha (HIF-1alpha) protein is rapidly degraded by the ubiquitin-proteasome system under normoxic conditions: its stabilization by hypoxia depends on redox-induced changes. *J Biol Chem* 1997;272:22642–7.
36. Maxwell PH, Wiesener MS, Chang GW, et al. The tumour suppressor protein VHL targets hypoxia-inducible factors for oxygen-dependent proteolysis. *Nature* 1999;399:271–5.
37. Zhong H, De Marzo AM, Laughner E, et al. Overexpression of hypoxia-inducible factor 1alpha in common human cancers and their metastases. *Cancer Res* 1999;59:5830–5.
38. Yang ZZ, Zhang AY, Yi FX, Li PL, Zou AP. Redox regulation of HIF-1alpha levels and HO-1 expression in renal medullary interstitial cells. *Am J Physiol Renal Physiol* 2003;284:F1207–15.
39. Krajewska M, Zapata JM, Meinhold-Heerlein I, et al. Expression of Bcl-2 family member Bid in normal and malignant tissues. *Neoplasia* 2002;4:129–40.
40. Fukazawa T, Walter B, Owen-Schaub LB. Adenoviral Bid overexpression induces caspase-dependent cleavage of truncated Bid and p53-independent apoptosis in human non-small cell lung cancers. *J Biol Chem* 2003;278:25428–34.
41. Zinkel SS, Ong CC, Ferguson DO, et al. Proapoptotic BID is required for myeloid homeostasis and tumor suppression. *Genes Dev* 2003;17:229–39.
42. Ryan HE, Lo J, Johnson RS. HIF-1 alpha is required for solid tumor formation and embryonic vascularization. *EMBO J* 1998;17:3005–15.
43. Banerjee SK, Zoubine MN, Sarkar DK, Weston AP, Shah JH, Campbell DR. 2-Methoxyestradiol blocks estrogen-induced rat pituitary tumor growth and tumor angiogenesis: possible role of vascular endothelial growth factor. *Anticancer Res* 2000;20:2641–5.
44. Sweeney CJ, Miller KD, Sissons SE, et al. The antiangiogenic property of docetaxel is synergistic with a recombinant humanized monoclonal antibody against vascular endothelial growth factor or 2-methoxyestradiol but antagonized by endothelial growth factors. *Cancer Res* 2001;61:3369–72.
45. Miller KD, Murry DJ, Curry E, et al. A phase 1 study of 2-methoxyestradiol plus docetaxel in patients with metastatic breast cancer [abstract]. Proceedings of the 38th Annual American Society of Clinical Oncology Meeting; 2002 May 18–21; Orlando, FL; American Society of Clinical Oncology, Alexandria, VA, 2002.
46. Basu A, Halder S. Identification of a novel Bcl-xL phosphorylation site regulating the sensitivity of Taxol- or 2-methoxyestradiol-induced apoptosis. *FEBS Lett* 2003;538:41–7.

Clinical Cancer Research

2-Methoxyestradiol Inhibits Hypoxia-Inducible Factor 1 α , Tumor Growth, and Angiogenesis and Augments Paclitaxel Efficacy in Head and Neck Squamous Cell Carcinoma

Justin L. Ricker, Zhong Chen, Xin Ping Yang, et al.

Clin Cancer Res 2004;10:8665-8673.

Updated version Access the most recent version of this article at:
<http://clincancerres.aacrjournals.org/content/10/24/8665>

Cited articles This article cites 43 articles, 22 of which you can access for free at:
<http://clincancerres.aacrjournals.org/content/10/24/8665.full#ref-list-1>

Citing articles This article has been cited by 7 HighWire-hosted articles. Access the articles at:
<http://clincancerres.aacrjournals.org/content/10/24/8665.full#related-urls>

E-mail alerts [Sign up to receive free email-alerts](#) related to this article or journal.

Reprints and Subscriptions To order reprints of this article or to subscribe to the journal, contact the AACR Publications Department at pubs@aacr.org.

Permissions To request permission to re-use all or part of this article, use this link
<http://clincancerres.aacrjournals.org/content/10/24/8665>.
Click on "Request Permissions" which will take you to the Copyright Clearance Center's (CCC) Rightslink site.